



# Hybrid Composite Membranes Based on Polyethylene Separator and Al<sub>2</sub>O<sub>3</sub> Nanoparticles for Lithium-Ion Batteries

Won-Kyung Shin, Yoon-Sung Lee, and Dong-Won Kim\*

Department of Chemical Engineering, Hanyang University, Seoul 133-791, Korea

A hybrid composite membrane is prepared by coating nano-sized Al<sub>2</sub>O<sub>3</sub> powder (13 and 50 nm) and poly(vinylidene fluoride-*co*-hexafluoropropene) (P(VdF-*co*-HFP)) binder on both sides of polyethylene separator. The composite membrane shows better thermal stability and improved wettability for organic liquid electrolyte than polyethylene separator, due to the presence of heat-resistant Al<sub>2</sub>O<sub>3</sub> particles with high-surface area in the coating layer. By using the composite membrane, the lithium-ion cells composed of carbon anode and LiNi<sub>1/3</sub>Co<sub>1/3</sub>Mn<sub>1/3</sub>O<sub>2</sub> cathode are assembled and their cycling performances are evaluated. The cells assembled with the composite membranes are proven to have better capacity retention than the cell prepared with polyethylene separator, due to the enhanced ability to retain the electrolyte solution in the cell. The cell assembled with the composite membrane containing 13 nm-sized Al<sub>2</sub>O<sub>3</sub> particles has an initial discharge capacity of 173.2 mA h g<sup>-1</sup> with good capacity retention.

**Keywords:** Al<sub>2</sub>O<sub>3</sub>, Composite Membrane, Li-Ion Battery, Nanoparticle.

IP: 163.152.17.113 On: Tue, 16 Apr 2013 07:11:51  
Copyright American Scientific Publishers

## 1. INTRODUCTION

Rechargeable lithium-ion batteries are being developed and produced as power sources for portable electronic devices, electric vehicles and energy storage systems due to their high energy density and long cycle life. In these batteries, a separator is a microporous membrane that prevents physical contact of the positive and negative electrodes while permitting ionic transport within the cell. It is a critical component to achieve good battery performance such as cycle life, energy density, high rate capability and safety.<sup>1,2</sup> Most of the separators used in lithium-ion batteries are based on microporous polyolefin membranes. Although the polyolefin membranes offer excellent mechanical strength and chemical stability, they exhibit large thermal shrinkage at high temperatures,<sup>3–5</sup> which causes a short circuit between electrodes in cases of unusual heat generation.

Separators should be also wet in the electrolyte solution and retain the electrolyte solution well. However, the large difference in polarity between the non-polar polyolefin separator and the highly polar organic electrolyte leads to poor wettability, which results in poor cycling stability.

Therefore, separators with enhanced thermal stability and good wettability in organic liquid electrolytes are highly desirable for the development of lithium-ion batteries with enhanced safety and good cycling performance. In this respect, the hybrid composite membranes that combine the characteristics of polymer separator and heat-resistant ceramic materials are being developed to achieve this goal.<sup>6–10</sup>

In this work, we tried to improve the thermal stability and wettability of a microporous polyethylene separator by coating both sides of the separator with nano-sized Al<sub>2</sub>O<sub>3</sub> particles and poly(vinylidene fluoride-*co*-hexafluoropropene) (P(VdF-*co*-HFP)) binder. It has been reported that the interfacial stability toward electrodes was improved when the nano-sized Al<sub>2</sub>O<sub>3</sub> was used as the filler.<sup>11</sup> The Al<sub>2</sub>O<sub>3</sub> could also hold the electrolyte solvent effectively and thus improved wettability for non-aqueous liquid electrolyte. Moreover, the composite membranes containing Al<sub>2</sub>O<sub>3</sub> particles exhibited good thermal stability, due to the presence of a heat-resistant alumina powder with a high surface area. With the composite membrane, we assembled lithium-ion cells composed of carbon anode and LiNi<sub>1/3</sub>Co<sub>1/3</sub>Mn<sub>1/3</sub>O<sub>2</sub> cathode. The cycling performances of cells with composite membranes were evaluated and compared to those of cell prepared with polyethylene separator.

\* Author to whom correspondence should be addressed.

## 2. EXPERIMENTAL DETAILS

### 2.1. Hybrid Composite Membrane

A hybrid composite membrane was prepared from nano-sized Al<sub>2</sub>O<sub>3</sub> powder (average particle size: 13 and 50 nm, Aldrich) and P(VdF-co-HFP) (Kynar 2801). P(VdF-co-HFP) and Al<sub>2</sub>O<sub>3</sub> powder (50:50 by weight) were dissolved in acetone and the solution was ball-milled for 48 h. The resulting viscous solution was cast with a doctor blade on to a microporous polyethylene separator (thickness: 20 μm, Asahi-Kasei Co.), then left so that the solvent evaporated at room temperature for 10 min. The solution was cast again on to the other side of the polyethylene separator. The Al<sub>2</sub>O<sub>3</sub>-coated separator was dried at room temperature for 10 min to allow the solvent to evaporate, followed by additional drying in a vacuum oven at 60 °C for 24 h. The thickness of hybrid composite membranes was measured to be 24 μm.

### 2.2. Electrode Preparation and Cell Assembly

The cathode consists of 85 wt.% LiNi<sub>1/3</sub>Co<sub>1/3</sub>Mn<sub>1/3</sub>O<sub>2</sub>, 7.5 wt.% PVdF, and 7.5 wt.% super-P carbon. The slurry of these materials was prepared in *N*-methyl pyrrolidone (NMP) and coated on aluminum foil. Its active mass loading corresponded to a capacity of about 1.0 mA h cm<sup>-2</sup>. The anode was also prepared by coating a NMP-based slurry of mesocarbon microbeads (MCMB), PVdF, and super-P carbon (85:7.5:7.5 by weight) on copper foil. The electrodes were roll pressed to enhance particulate contact and adhesion to the current collector. Lithium-ion cells were assembled by sandwiching the composite membrane between the carbon anode and the LiNi<sub>1/3</sub>Co<sub>1/3</sub>Mn<sub>1/3</sub>O<sub>2</sub> cathode. The cell was then enclosed in a pouch bag injected with the electrolyte solution. The electrolyte used was 1.15 M LiPF<sub>6</sub> in ethylene carbonate (EC)/diethyl carbonate (DEC) (3:7 by volume, Techno Semichem Co. Ltd.). All cells were assembled in a dry box filled with argon gas.

### 2.3. Measurements

The surface morphologies of polyethylene separator and hybrid composite membranes were examined using a field emission scanning electron microscope (FE-SEM) (JEOL, JSM-6330F). The porosity ( $\varphi$ ) of the coating layer on polyethylene separator was measured by the equation given in previous studies,<sup>12–14</sup>

$$\varphi = 1 - \rho_m / \rho_t \quad (1)$$

where  $\rho_m$  and  $\rho_t$  are the measured density and theoretical density of coating layer, respectively. Thermal shrinkage of the composite membrane in the form of dimensional change was measured before and after being kept at 105 °C for 1 hr. In order to measure electrolyte uptake and ionic

conductivity, the composite membrane was first immersed in LiPF<sub>6</sub> in EC/DEC for 1 hr. Afterward, it was taken out from the electrolyte solution and excess electrolyte solution on the surface of membrane was removed by wiping with filter paper. The uptake of electrolyte solution was determined using the following Eq. (2),

$$\text{uptake (\%)} = (W - W_o) / W_o \times 100 \quad (2)$$

where,  $W_o$  and  $W$  are the weights of the membrane before and after soaking in the liquid electrolyte, respectively.<sup>15–17</sup> The wetted membrane was sandwiched between two stainless steel electrodes for conductivity measurements. The cell was enclosed in a pouch bag and sealed to permit testing outside of a glove box. AC impedance measurements were performed to measure ionic conductivity using an impedance analyzer over the frequency range of 10 Hz to 100 kHz with amplitude of 10 mV. Charge and discharge cycling tests of the lithium-ion cells were conducted at a current density of 0.5 mA cm<sup>-2</sup> (0.5 C rate) over a voltage range of 3.0–4.5 V with battery test equipment at room temperature and 55 °C.

## 3. RESULTS AND DISCUSSION

FE-SEM images of the surface of microporous polyethylene separator and hybrid composite membranes are presented in Figure 1. The polyethylene separator exhibits a uniformly interconnected submicron pore structure. As the nano-sized Al<sub>2</sub>O<sub>3</sub> powder with P(VdF-co-HFP) binder was coated onto the polyethylene separator, the ceramic particles were covered the polymer binder. The porosities of the coating layer on polyethylene separator were measured to be 0.56 and 0.62 for the composite membrane containing 13 and 50 nm-sized Al<sub>2</sub>O<sub>3</sub> particles, respectively. The presence of porous coating layer consisting of Al<sub>2</sub>O<sub>3</sub> powder with P(VdF-co-HFP) may improve the thermal stability of the polyethylene separator and also lead to efficient gelation by liquid electrolyte when it is immersed in an electrolyte solution.

In order to evaluate the heat-resistant properties of the hybrid composite membranes, we measured thermal shrinkage after storing them at 105 °C for 1 hr, and the results are given in Table I. The polyethylene separator shows a high degree of shrinkage after exposure to the high temperature. Since the manufacturing process of polyethylene separator includes a drawing step, they shrink easily when exposed to high temperature, due to internal stress.<sup>2</sup> Consequently the polyethylene separator loses mechanical stability upon exposure to high temperatures, which can result in internal short between anode and cathode in lithium-ion batteries. It can be seen that the thermal shrinkage is significantly reduced by coating the polyethylene separator with nano-sized Al<sub>2</sub>O<sub>3</sub> powder and P(VdF-co-HFP) binder. It is considered that coating of heat-resistant ceramic particles onto both sides of the polyethylene separator can prevent dimensional changes

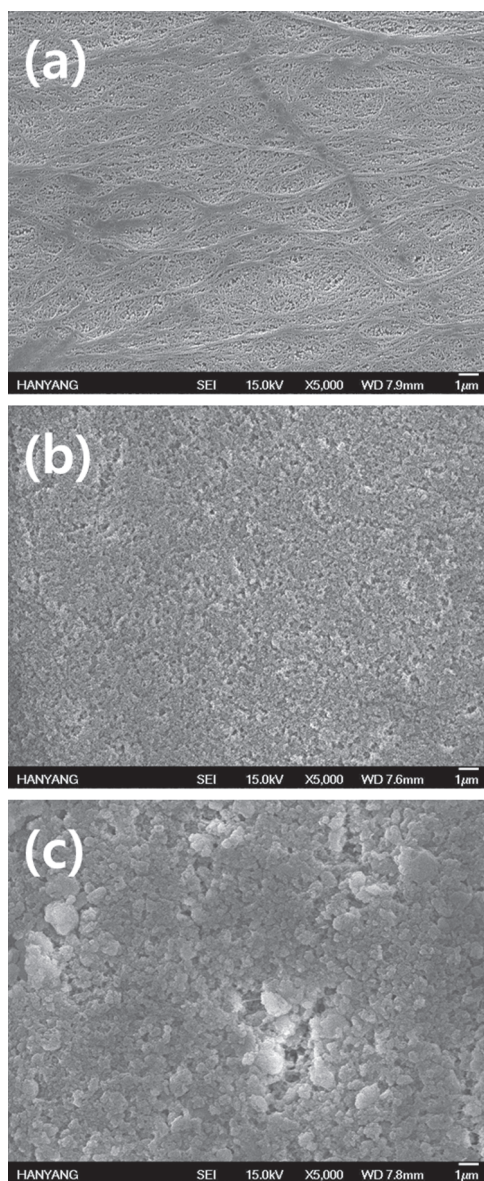


**Fig. 1.** FE-SEM images of the surface of polyethylene separator and composite membranes. (a) Polyethylene separator, (b) composite membrane containing Al<sub>2</sub>O<sub>3</sub> with a particle size of 13 nm, (c) composite membrane containing Al<sub>2</sub>O<sub>3</sub> with a particle size of 50 nm.

by thermal deformation because of the frame structure of the heat-resistant ceramic powder with polymer binder. The improvement of thermal stability is more remarkable when the Al<sub>2</sub>O<sub>3</sub> powders with particle size of 13 nm are used (thermal shrinkage is 3.4%). This result may originate from their large surface area and high volume ratio to polymer binder. Electrolyte uptake and ionic conductivity of composite membranes are also summarized in Table I. As expected, the polyethylene separator exhibits poor wettability due to its inherent hydrophobic characteristics. For the composite membranes, the amount of electrolyte absorbed is greater than the amount absorbed by polyethylene separator, which results in higher ionic

**Table I.** Thermal shrinkage, electrolyte uptake and ionic conductivities of polyethylene separator and composite membranes.

Membrane	Thickness (μm)	Thermal shrinkage (%)	Electrolyte uptake (%)	Ionic conductivity (S cm <sup>-1</sup> )
PE separator	20	9.8	93.8	2.2 × 10 <sup>-4</sup>
Composite membrane (Φ = 13 nm)	24	3.4	183.3	4.0 × 10 <sup>-4</sup>
Composite membrane (Φ = 50 nm)	24	3.9	152.1	3.5 × 10 <sup>-4</sup>

conductivity. This result can be ascribed to the presence of the nano-sized Al<sub>2</sub>O<sub>3</sub> particles with high-surface area. In addition, since P(VdF-co-HFP) is a copolymer that is easily swollen by an electrolyte solution, a higher amount of electrolyte solution is expected to be retained by the polymer binder.

Ionic conductivities of different membranes soaked in electrolyte solution were measured as a function of storage time. Figure 2 illustrates the time dependence of the ionic conductivity for the electrolytes prepared with polyethylene separator and composite membranes, respectively. As discussed above, the electrolytes prepared with the composite membranes exhibit higher ionic conductivity than polyethylene separator over time periods measured. It should be noted that ion conduction behavior with time is different for each parent membrane. Gradual decrease in the ionic conductivity for polyethylene separator may be related to the solvent exudation upon long storage, which arising from poor compatibility with electrolyte solution. After conductivity measurements, liquid electrolyte exuding from the polyethylene separator was observed in the cell. On the contrary, constant values of ionic conductivity for the composite membranes for a long period of time suggest that the electrolyte solution is well encapsulated in the composite membrane.

Cycling performance of lithium-ion cells prepared with the composite membranes was evaluated. All cells were

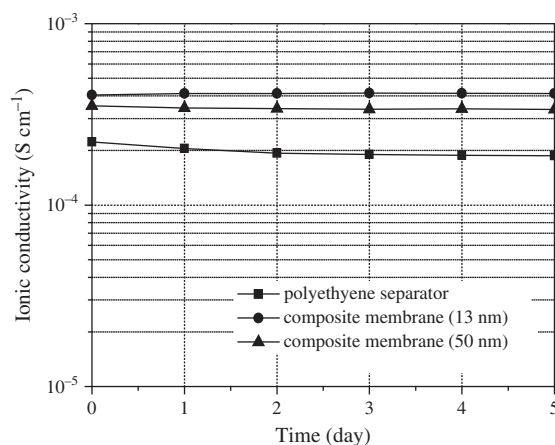


**Fig. 2.** Time evolution of the ionic conductivity of polyethylene separator and composite membranes soaked in LiPF<sub>6</sub> in EC/DEC.

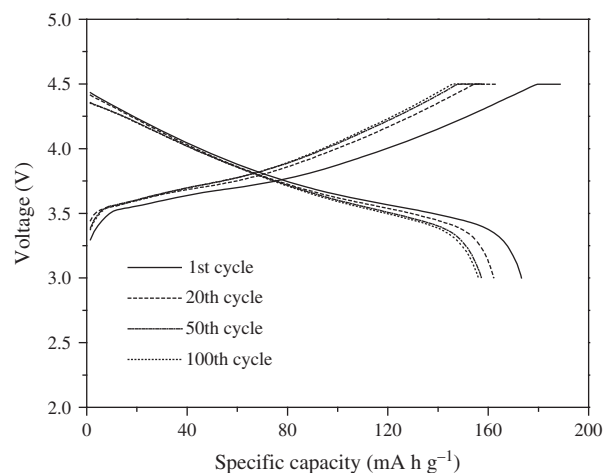


**Fig. 3.** Charge and discharge curves of lithium-ion cell assembled with the composite membrane containing 13 nm-sized Al<sub>2</sub>O<sub>3</sub> particles. (0.5 C CC and CV charge, 0.5 C CC discharge, cut-off: 3.0–4.5 V.)

charged at a current density of 0.5 mA cm<sup>-2</sup> (0.5 C rate) up to a target voltage of 4.5 V. This was followed by a constant voltage charge with a decline of current until a final current was reached to 20% of the charging current. The cells were then discharged to a cut-off voltage of 3.0 V at the same current density (0.5 C rate). Figure 3 shows the charge–discharge curves of the 1st, 20th, 50th and 100th cycle of the lithium-ion cell assembled with the composite membrane containing 13 nm-sized Al<sub>2</sub>O<sub>3</sub> particles. The cell delivers an initial discharge capacity of 173.2 mA h g<sup>-1</sup> based on active LiNi<sub>1/3</sub>Co<sub>1/3</sub>Mn<sub>1/3</sub>O<sub>2</sub> material in the cathode. After 100 cycles, the discharge capacity of the cell declines to 156.1 mA h g<sup>-1</sup>, which corresponds to 90.1% of the initial discharge capacity.

Figure 4 compares the discharge capacities of lithium-ion cells assembled with different membranes, as a function

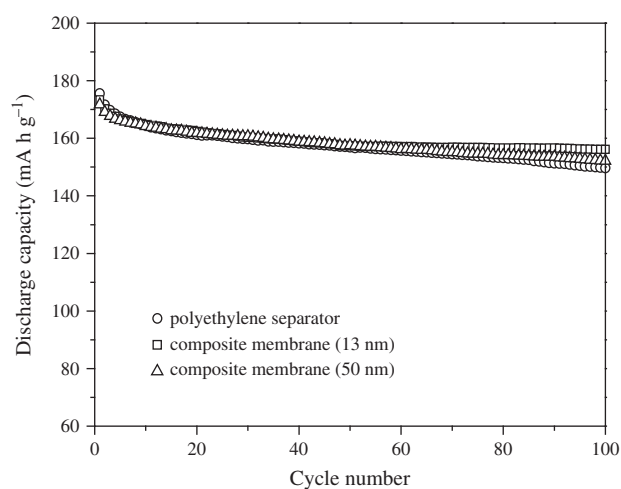


**Fig. 4.** Discharge capacities of the lithium-ion cells prepared with polyethylene separator and composite membranes, as a function of cycle number. (0.5 C CC and CV charge, 0.5 C CC discharge, cut-off: 3.0–4.5 V.)

of cycle number. The cycling characteristics of the cells are found to depend on the type of membrane. The initial discharge capacity of the cell is slightly decreased by coating the polyethylene separator with Al<sub>2</sub>O<sub>3</sub> powder and polymer binder. Presence of an additional coating layer on the porous polyethylene separator may increase the resistance of ion migration in the cell, giving rise to a reduced discharge capacity. On the other hand, the capacity retention is improved by coating Al<sub>2</sub>O<sub>3</sub> powder and polymer binder. As discussed in Figure 2, the ability to retain electrolyte solution in the composite membrane is higher than in the hydrophobic polyethylene separator alone, and thus helps to prevent a lack or leak of electrolyte during repeated cycling. When examining the effect of the particle size of Al<sub>2</sub>O<sub>3</sub> powder on the cell performance, the cell assembled with composite membrane containing 13 nm-sized Al<sub>2</sub>O<sub>3</sub> powder exhibits better capacity retention. The ability to retain the electrolyte solution in the composite membrane was favored by using smaller Al<sub>2</sub>O<sub>3</sub> powders with high surface area, which helped to prevent release of electrolyte solution during cycling. The stable interfacial characteristics promoted by the fine Al<sub>2</sub>O<sub>3</sub> particles due to their large surface area and high volume may also have contributed to the improved capacity retention, as reported earlier.<sup>18–20</sup>

Rate capability of the lithium-ion cell prepared with the composite membrane was evaluated. Cells were charged to 4.5 V at a constant current of 0.1 C and discharged at different current rates ranging from 0.1 C to 2.0 C. Figure 5 shows the relative discharge capacities of lithium-ion cells assembled with different membrane, as a function of current rate. Here, the relative capacity is defined as the ratio of the discharge capacity at a specific C rate to the discharge delivered at a rate of 0.1 C. The cells assembled with composite membrane show slightly lower capacity at high current rate, as compared to the cell prepared with polyethylene separator.

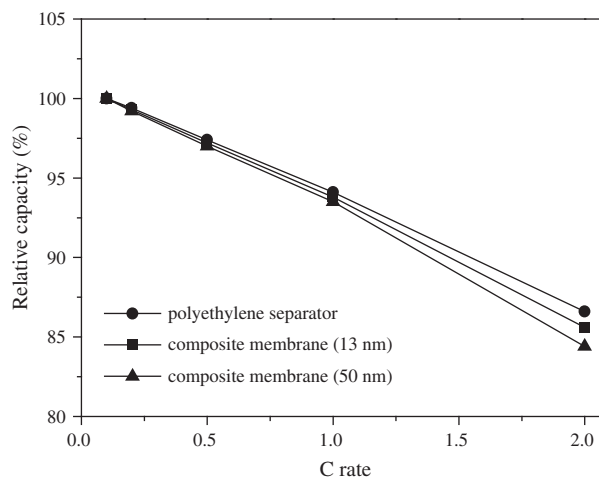


**Fig. 5.** Relative capacities of lithium-ion cells prepared with polyethylene separator and composite membranes, as a function of C rate.



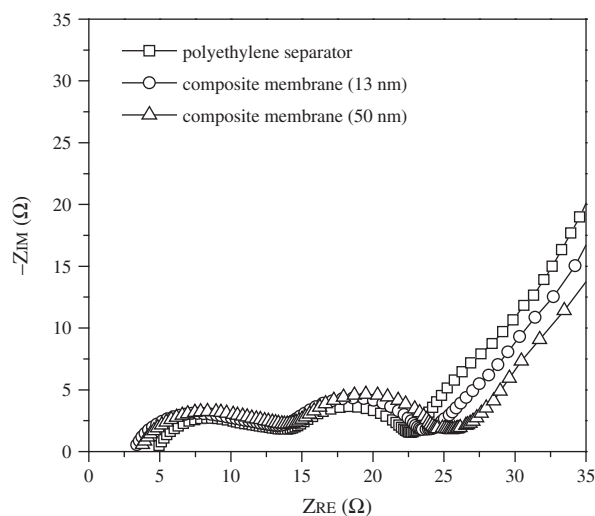


**Fig. 6.** AC impedance spectra of the lithium-ion cells assembled with polyethylene separator and composite membranes, which are measured after cycling.

In order to investigate the origin for difference in high rate performance, the ac impedance of the cells was measured after evaluating the rate capability. The resultant ac impedance spectra exhibiting two semicircles are shown in Figure 6. According to previous ac impedance analysis,<sup>21,22</sup> the semicircle in the high frequency range can be attributed to the resistance due to Li<sup>+</sup> ion migration through the surface film on the electrode and the semicircle in the medium to low frequency range is due to charge transfer resistance between the electrode and electrolyte. The surface film resistance observed in the high frequency region was hardly affected by the type of membrane. On the other hand, the charge transfer resistance was found to be higher in the cell assembled with the composite membrane. This result suggest that the coating layer composed of nano-sized Al<sub>2</sub>O<sub>3</sub> powder and P(VdF-co-HFP) binder in the composite membrane may hamper the charge transfer reaction in the cell even if the coating layer on the polyethylene separator can improve the wettability towards electrolyte solution.

Cycling performances of the lithium-ion cells prepared with the polyethylene separator and composite membranes were evaluated at high temperature (55 °C), and the results are shown in Figure 7. The initial discharge capacity of the cell was irrespective of the membrane used in lithium-ion cells, as shown in Figure 7(a). Also, the difference in high rate performance was not noticeable, as depicted in Figure 7(b). These results suggest that an additional coating layer on the porous polyethylene separator hardly affects the internal resistance of the cell, as the temperature increased. However, the effect of type of the membrane on the capacity retention was more significant at high temperature than room temperature (Fig. 4). This result indicates that the ability to retain electrolyte solution in the cell is more prominent at high temperature, because the coating

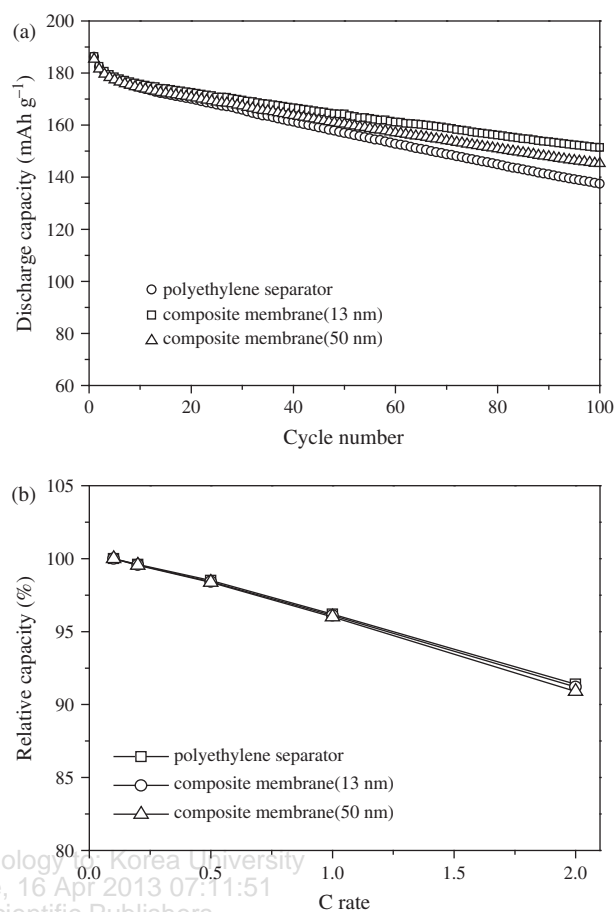


**Fig. 7.** (a) Discharge capacities with cycle number and (b) rate capability of the lithium-ion cells prepared with polyethylene separator and composite membranes, which are measured at 55 °C.

layer gelled by liquid electrolyte may prevent a lack or leak of electrolyte solution during repeated cycling.

#### 4. CONCLUSION

Nano-sized Al<sub>2</sub>O<sub>3</sub> particle and P(VdF-co-HFP) binder were coated on both sides of polyethylene separator to prepare a composite membrane. The composite membranes exhibited enhanced thermal stability by retaining stable dimensions at high temperature. Due to the high hydrophilicity of the P(VdF-co-HFP) and high surface area of nano-sized Al<sub>2</sub>O<sub>3</sub> particle, the composite membranes encapsulated higher amounts of electrolyte solution, as compared to polyethylene separator. As a result, the lithium-ion cell assembled with the composite membrane containing 13 nm-sized Al<sub>2</sub>O<sub>3</sub> powder exhibited better capacity retention than did the cell prepared with a polyethylene separator. The use of composite the membrane significantly enhanced the capacity retention at high temperature, due to the effective gelation of liquid electrolyte by coating layer, which prevents a lack or leak of electrolyte solution during repeated cycling.

**Acknowledgment:** This work was supported by the National Research Foundation (NRF) of Korea Grant, funded by the Korea government (MEST) (NRF-2009-C1AAA001-0093307). This research was also supported by a Grant from the Fundamental R&D Program for Core Technology of Materials, funded by the Ministry of Knowledge Economy, Korea.

## References and Notes

1. P. Arora and Z. Zhang, *Chem. Rev.* 104, 4419 (2004).
2. S. S. Zhang, *J. Power Sources* 164, 351 (2007).
3. G. Venugopal, J. Moore, J. Howard, and S. Pandalwar, *J. Power Sources* 77, 34 (1999).
4. I. Uchida, H. Ishikawa, M. Mohamedi, and M. Umeda, *J. Power Sources* 119, 821 (2003).
5. M. S. Wu, P. C. J. Chiang, J. C. Lin, and Y. S. Jan, *Electrochim. Acta* 49 1830 (2004).
6. S. Augustin, V. D. Hennige, G. Horpel, and C. Hying, *Desalination* 146, 23 (2002).
7. P. Kritzer, *J. Power Sources* 161, 1335 (2006).
8. N. T. Kalyana Sundaram, and A. Subramania, *Electrochim. Acta* 52, 4987 (2007).
9. J. A. Choi, S. H. Kim, and D. W. Kim, *J. Power Sources* 195, 6192 (2010).
10. J. H. Park, W. Park, J. H. Kim, D. Ryoo, H. S. Kim, Y. U. Jeong, D. W. Kim, and S. Y. Lee, *J. Power Sources* 196, 7035 (2011).
11. C. M. Yang, H. S. Kim, B. K. Na, K. S. Kum, and B. W. Cho, *J. Power Sources* 156, 574 (2006).
12. T. Michot, A. Nishimoto, and M. Watanabe, *Electrochim. Acta* 45, 1347 (2000).
13. A. Magistris, P. Mustarelli, F. Parazzoli, E. Quartarone, P. Piaggio, and A. Bottino, *J. Power Sources* 97–98, 657 (2001).
14. D. W. Kim, K. A. Noh, H. S. Min, D. W. Kang, and Y. K. Sun, *Electrochem. Solid-State Lett.* 5, A63 (2002).
15. J. R. Kim, S. W. Choi, S. M. Jo, W. S. Lee, and B. C. Kim, *J. Electrochem. Soc.* 152, A295 (2005).
16. X. Li, G. Cheruvally, J. K. Kim, J. W. Choi, J. H. Ahn, K. W. Kim, and H. J. Ahn, *J. Power Sources* 167, 491 (2007).
17. Y. Ding, P. Zhang, Z. Long, Y. Jiang, F. Xu, and W. Di, *J. Membr. Sci.* 329, 56 (2009).
18. M. C. Borghini, M. Mastragostino, S. Passerini, and B. Scrosati, *J. Electrochem. Soc.* 142, 2118 (1995).
19. J. Fan and P. S. Fedkiw, *J. Electrochem. Soc.* 144, 399 (1997).
20. F. Croce, G. B. Appetecchi, L. Persi, and B. Scrosati, *Nature* 394, 456 (1998).
21. A. Funabiki, M. Inaba, and Z. Ogumi, *J. Power Sources* 68, 227 (1997).
22. M. D. Levi, G. Salitra, B. Markovsky, H. Teller, D. Aurbach, U. Heider, and L. Heider, *J. Electrochem. Soc.* 146, 1279 (1999).

Received: 4 November 2011. Accepted: 11 June 2012.

Delivered by Publishing Technology to: Korea University  
IP: 163.152.17.113 On: Tue, 16 Apr 2013 07:11:51  
Copyright American Scientific Publishers